Physics of the Solid State, 2025, Vol. 67, No. 11

15,11

Nuclear Magnetic Resonance Study of Lithium Diffusion in Intercalated Titanium Diselenides

© R.V. Skoryunov[1], O.A. Babanova[1,2], A.V. Soloninin[1], A.N. Titov[1], O.V. Bushkova[3], A.V. Skripov[1]

[1] M.N. Mikheev Institute of Metal Physics of Ural Branch of Russian Academy of Sciences,
Yekaterinburg, Russia
[2] Ural Federal University after the first President of Russia B.N. Yeltsin,
Yekaterinburg, Russia
[3] Institute of Solid State Chemistry, Ural Branch of Russian Academy of Sciences,
Yekaterinburg, Russia

E-mail: skoryunov@imp.uran.ru

Received July 18, 2025
Revised July 18, 2025.
Accepted November 12, 2025

To study the dynamical properties of intercalated compounds Li_xTiSe_2 ($x = 0.25, 1$), we have measured the ^{7}Li nuclear magnetic resonance spectra and spin-lattice relaxation rates in these compounds over the temperature range of (80−593 K). It has been shown that the behavior of the spin-lattice relaxation rates above 300 K is determined by quasi-two-dimensional translational diffusion of Li^+ ions. The diffusion of lithium in $Li_{0.25}TiSe_2$ is characterized by the activation energy of 501(28) meV, and in $LiTiSe_2$ by the activation energy of 509(15) meV. The diffusion coefficients and ionic conductivity of Li^+ in both $Li_{0.25}TiSe_2$ and $LiTiSe_2$ have been estimated at 297 K.

Keywords: spin-lattice-relaxation, layered dichalcogenides, atomic motion, quasi-2D diffusion, cathode materials.

DOI: 10.61011/PSS.2025.11.62971.203-25

1. Introduction

Layered dichalcogenides of transition metals attracted attention due to their ability to accept various organic and inorganic objects into their interlayer space (intercalation) [1–4]. Such compounds with the general formula MX_2 (M = transition metal, X = S, Se, Te) create the structures that consist of X−M−X layers held together with Van der Waals forces. It is known that layered dichalcogenides may be intercalated by different materials without a substantial change to the structures of source compounds [5,6]. As a result of intercalation of alkali metals, a charge (electron) transfer occurs between the intercalated atoms and X−M−X layers that causes replacement of Van der Waals forces with Coulomb interaction. The source lattice after intercalation changes slightly along the crystallographic axis c (the distance between the layers increases) [7].

Different classes of layered dichalcogenide have a wide spectrum of practical application, for example, are used to develop electrodes, solid-state ion conductors and semiconductor materials [2,3]. Lithium-intercalated dichalcogenides Li_xMX_2 are seen as the promising compounds to develop cathode materials. In particular, the compounds of Li_xTiS_2 type were actively studied with the purpose of their potential use as cathode materials for lithium batteries [2,6,8]. Titanium diselenide $TiSe_2$ is a compound that is related to titanium disulfide TiS_2, and recent research of lithium-intercalated compounds of Li_xTiSe_2 type also demonstrated the possibility of using these compounds as ion conductors [9,10]. Apart from the applied use, compounds of Li_xTiSe_2 type attract attention as the models to study the motion mechanisms of objects intercalated into layered dichalcogenides. Nuclear magnetic resonance (NMR) has proven to be an effective method to obtain information at a microlevel on the atomic dynamics in solids, such as cation mobility in lithium-ion conductors [11,12]. In the present work ^{7}Li NMR spectra and spin-lattice relaxation rates we measured to study the dynamic properties of Li^+ in Li_xTiSe_2 ($x = 0.25, 1$) compounds in a wide temperature range.

2. Experimental details

Li_xTiSe_2 compounds were synthesized in the manner similar to that described in paper [13]. According to the X-ray diffraction data, the compounds have trigonal symmetry (space group P-3m1) with the lattice parameters: $a = 3.6027(1)$ Å and $c = 6.4663(2)$ Å for $LiTiSe_2$ [13], $a = 3.5542(5)$ Å and $c = 6.1142(16)$ Å for $Li_{0.25}TiSe_2$ [13]. A schematic representation of this structure is shown in Figure 1. For NMR-experiments the powder samples were sealed into pyrex ampoules under vacuum of 10^{-5} Torr.

^{7}Li NMR-experiments were conducted on a pulse spectrometer with quadrature phase detection in resonance frequencies $\omega/2\pi = 14.8$ and 28 MHz in the temperature interval of 80−593 K. The magnetic field was developed using an electromagnet by Bruker company. To stabilize the magnetic field, a polynuclear NMR magnetometer of in-house production was used that operated in the range of 0.32−2.15 T. To generate radiofrequency pulses, a computer

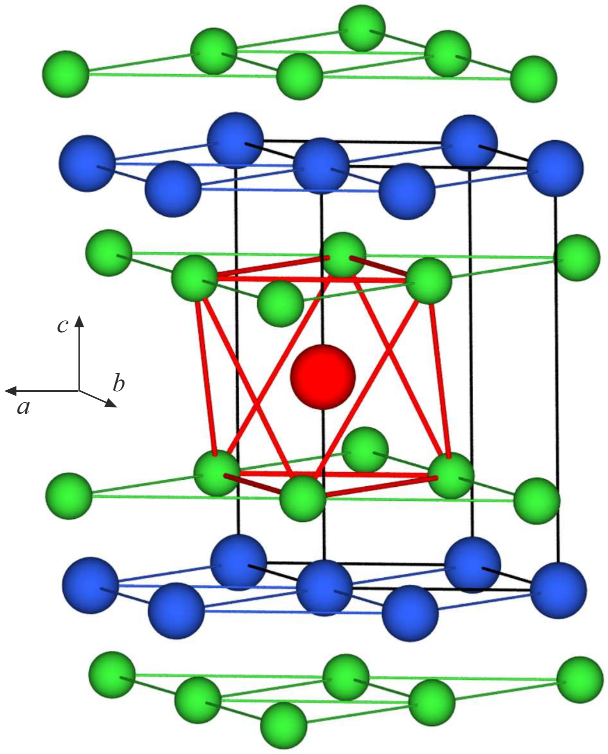

Figure 1. Schematic representation of the structure Li_xTiSe_2. Red is for Li atoms, blue — for Ti, green — for Se.

pulse programmator SpinCore, a PTS (Programmed Test Sources, Inc.) frequency synthesizer and a broadband pulse amplifier Kalmus with capacity of 1 kW were used. The typical duration of 90°th pulse was 5–6 μs. For measurements at temperatures of $T \leq 300$ K a resonance probe with a sample was placed into a continuous-flow cryostat Oxford Instruments CF1200, which used helium or nitrogen as a refrigerant. The sample temperature was monitored using a chromel-alumel thermocouple with the accuracy of ±0.1 K. Measurements at temperatures of $T > 300$ K were carried out using a resonance probe with a built-in furnace, where the temperature was controlled with a copper-constantan thermocouple with the accuracy of ±0.5 K. To measure nuclear spin-lattice relaxation rates, the „saturation–recovery“ method was used. NMR spectra were recorded via Fourier transform of solid-echo signals (pulse sequence $\pi/2_x - t - \pi/2_y$).

3. Results and discussion

The main features of the recorded ^{7}Li NMR spectra were the same for both studied compounds. As an example, Figure 2 shows the evolution of ^{7}Li MNR spectra with temperature for $LiTiSe_2$, measured at the frequency of 28 MHz. At low temperatures the width $\Delta\nu$ (full width at half maximum) of the ^{7}Li NMR spectrum is defined by dipole-dipole interaction between the static nuclear spins. This parameter is called the width of the „rigid lattice“ line $\Delta\nu_R$. As temperature increases, the width of the „rigid lattice“ line starts decreasing as a result of averaging of dipole-dipole interactions, when the frequency of lithium atoms jumps, τ^{-1}, becomes approximately equal to the value $2\pi\Delta\nu_R$ [14]. In the studied compounds the substantial narrowing of the line happens at the temperature, when τ^{-1} reaches around $10^4\,s^{-1}$. At low temperatures the shape of the ^{7}Li NMR spectrum for $LiTiSe_2$ also has characteristic „wings“, which may be related to the unresolved quadrupole satellites.

Figure 3 shows temperature dependences of width $\Delta\nu_{Li}$ of NMR spectra measured in a ^{7}Li nucleus in $Li_{0.25}TiSe_2$ and $LiTiSe_2$. Behavior of $\Delta\nu_{Li}(T)$ in both samples is typical for the compounds with the translational diffusion of ions Li^+ [15–17]. From Figure 3 you can see that the substantial narrowing of the NMR line starts at temperatures of 300 K in $Li_{0.25}TiSe_2$ and 350 K in $LiTiSe_2$. In the area

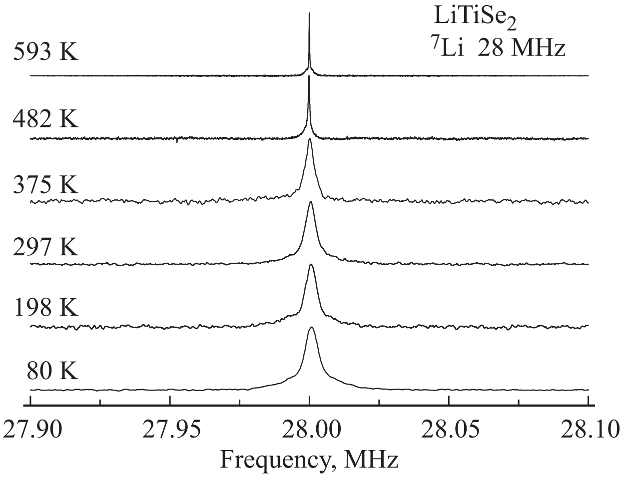

Figure 2. Evolution of ^{7}NMR spectra for $LiTiSe_2$ with temperature.

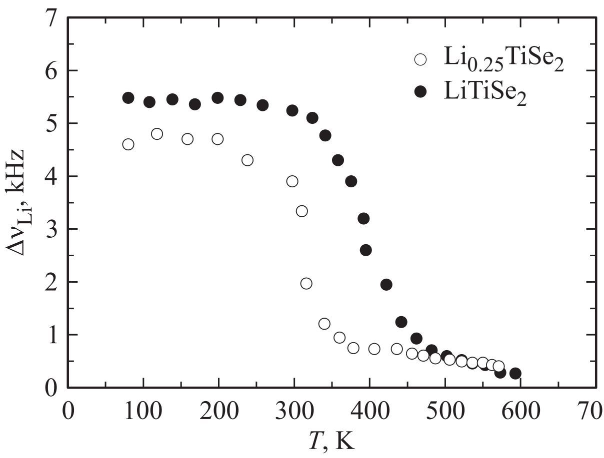

Figure 3. Temperature dependence of width (full width at half maximum) of the NMR spectrum measured at a ^{7}Li nucleus, in $Li_{0.25}TiSe_2$ and $LiTiSe_2$ at frequency of 28 MHz.

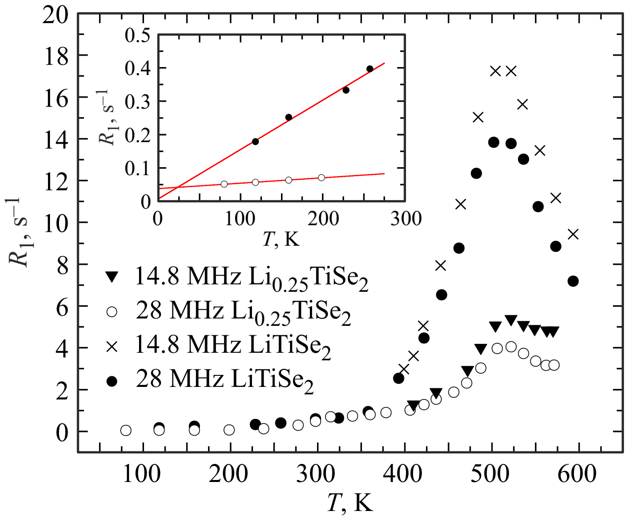

Figure 4. Temperature dependences of spin-lattice relaxation rates in ^{7}Li nucleus measured at frequencies of 14.8 and 28 MHz for $Li_{0.25}TiSe_2$ and $LiTiSe_2$. The insert shows the behavior of relaxation rates below $T = 300$ K, and red lines show linear approximations of $C_eT + B$ for each compound.

of high-temperature plateau the $\Delta\nu_{Li}$ values are very low (~ 0.37 kHz for $Li_{0.25}TiSe_2$ and ~ 0.26 kHz for $LiTiSe_2$ at 570 K), which indicates practically complete averaging of dipole-dipole interaction ^{7}Li–^{7}Li. Such $\Delta\nu_{Li}$ behavior is observed in case of translational diffusion. It should be noted that despite isostructurality of compounds, the width of the line in $Li_{0.25}TiSe_2$ is less in the low temperature area than in $LiTiSe_2$, which may be explained by the difference of dipole-dipole interaction ^{7}Li–^{7}Li due to different concentration of ions Li$^+$ in the systems [14]. Narrowing of the line in $Li_{0.25}TiSe_2$ happens at lower temperature than in $LiTiSe_2$. This fact means that atomic jumps of lithium in $Li_{0.25}TiSe_2$ at the frequency scale $\sim 10^4\,s^{-1}$ start at lower temperature compared to $LiTiSe_2$. The data from Figure 3 may be compared to the behavior of the NMR line width ^{7}Li for $Li_{0.7}TiSe_2$ measured at 77.7 MHz [18]. In general, the $\Delta\nu_{Li}(T)$ behavior for $Li_{0.7}TiSe_2$ agrees with the results we obtained for $Li_{0.25}TiSe_2$ and $LiTiSe_2$. The only difference is the fact that in $Li_{0.7}TiSe_2$ the line starts narrowing due to atomic motion around the temperature of 200 K, at which τ^{-1} reaches the value of the order of $10^4\,s^{-1}$ [18]. Probably, this is related to lower energy barriers for atomic motion of lithium in $Li_{0.7}TiSe_2$ compared to barriers in $Li_{0.25}TiSe_2$ and $LiTiSe_2$.

Temperature dependences of the measured spin-lattice relaxation rates ^{7}Li (in exponential approximation) at frequencies of 14.8 and 28 MHz for $Li_{0.25}TiSe_2$ and $LiTiSe_2$ samples are presented in Figure 4. It should be noted that the measured spin-lattice relaxation rates R_1 is usually determined by the sum of contributions from interaction of nuclear spins with conductivity electrons (R_{1e}), with paramagnetic impurities (R_{1p}), and from internuclear dipole-dipole and electric quadrupole interactions modulated by atomic motion (R_{1d}) [19]. The contribution from conductivity electrons (Korringa contribution) R_{1e} is proportionate to temperature and does not depend on frequency, $R_{1e} = C_eT$. In paramagnetics the electron contribution to the spin-lattice relaxation rates dominates at low temperatures, whereas the contribution caused by atomic motion R_{1d} becomes dominant in the temperature range, at which the frequency of atomic jumps τ^{-1} stays within 10^7–$10^{11}\,s^{-1}$. From the insert in Figure 4 you can see that the measured temperature dependence of relaxation rate at $T < 300$ K may be described satisfactorily by linear function $C_eT + B$ with parameters $C_e = 1.62 \cdot 10^{-4}\,s^{-1}K^{-1}$ and $B = 3.79 \cdot 10^{-2}\,s^{-1}$ for $Li_{0.25}TiSe_2$ and $C_e = 1.48 \cdot 10^{-3}\,s^{-1}K^{-1}$ and $B = 7.17 \cdot 10^{-3}\,s^{-1}$ for $LiTiSe_2$. The C_e coefficient is proportionate to the squared density of electron states at the Fermie level [19]. The B parameter defines the paramagnetic contribution R_{1p} within low temperatures. To assess the Li$^+$ motion parameters, we have to identify the temperature dependence of the contribution created by atomic motion R_{1d}, i. e. subtract R_{1e} and R_{1p} contributions from the experimental data. This procedure is usually based on the extrapolation of low-temperature data $C_eT + B$ [20].

The analysis of our experimental results found that in both compounds the recovery of nuclear magnetization of ^{7}Li deviates from the exponential behavior. In the considered temperature range the ^{7}Li recovery curves may be satisfactorily approximated by the sum of two exponential functions. Biexponential relaxation of ^{7}Li was already observed previously in some compounds that contain lithium [16]. Such behavior may be related to non-zero electric quadrupole moment of ^{7}Li nucleus [14]. Figure 5, *a* and 5, *b* show the behavior of fast components of spin-lattice relaxation rates R_{1F}^{Li}, related to atomic motion, on ^{7}Li nucleus, measured at two resonance frequencies for $Li_{0.25}TiSe_2$ and $LiTiSe_2$, accordingly, depending on inverted temperature. The considerable spread of points in the chart may refer to a certain instability of biexponential description of recovery curves. The frequency-dependent peak R_1^{Li} is observed at the temperature of 463 K for $Li_{0.25}TiSe_2$ and 475 K for $LiTiSe_2$ at the frequency of 14.8 MHz. Such peak is typical for contributions to the spin-lattice relaxation rates caused by atomic motion [14]. The maximum of spin-lattice relaxation rate must be observed at temperature, at which the frequency of atomic jumps τ^{-1} becomes approximately equal to the resonance frequency ω. Taking into account the behavior of the ^{7}Li NMR line width (see Figure 3), you can state that this maximum R_1^{Li} confirms our assumption on the existence of translational diffusion of Li$^+$ ions in both compounds.

According to the standard theory of spin-lattice relaxation caused by atomic motion [14], within slow motions (low-temperature slope, where $\omega\tau \gg 1$), R_{1F}^{Li} must be proportionate to $\omega^{-2}\tau^{-1}$, and within fast motions (high-temperature slope, where $\omega\tau \ll 1$) it is proportionate to τ and does not depend on frequency. However, from Figure 5, *a* and 5, *b* you can see that the frequency

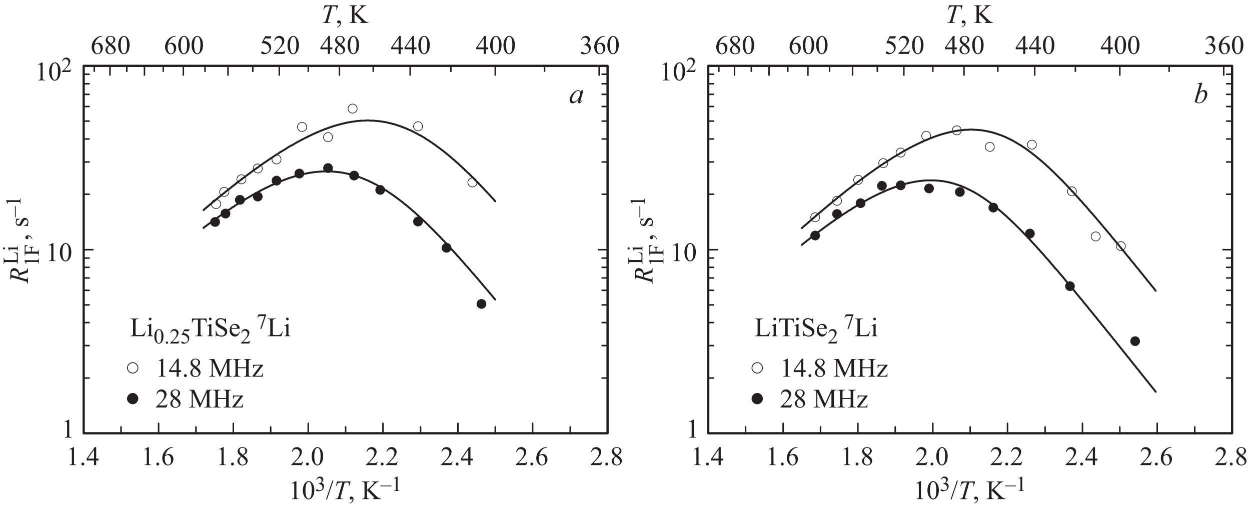

Figure 5. Spin-lattice relaxation rates components in ^{7}Li nucleus related to atomic motion and measured at frequencies of 14.8 and 28 MHz in $Li_{0.25}TiSe_2$ (*a*) and $LiTiSe_2$ (*b*), depending on inverted temperature. Solid lines show approximation of data by the model for quasi-two-dimensional diffusion.

Parameters of atomic motion obtained with a model for quasi-two-dimensional diffusion

Compound	E_a (meV)	τ_0 (s)	ΔM (s^{-2})
$Li_{0.25}TiSe_2$	501 ± 28	$(1.90 \pm 0.16) \cdot 10^{-14}$	$(5.9 \pm 0.2) \cdot 10^9$
$LiTiSe_2$	509 ± 15	$(2.20 \pm 0.12) \cdot 10^{-14}$	$(5.2 \pm 0.2) \cdot 10^9$

dependence remains at the high-temperature slope, even though it becomes weaker that in the low-temperature slope. Such feature of the behavior may be explained within low-dimensional diffusion [21]. It is well known that the spin-lattice relaxation rates do not depend on resonance frequency within fast motions only in case of isotropic (3D) atomic diffusion, whereas in the case of low-dimensional (quasi-1D, quasi-2D) translational diffusion the frequency dependence stays at the high-temperature slope [21]. Since $TiSe_2$ is a layered dichalcogenide, and lithium in both compounds was intercalated between the layers, we can assume that in this case there is indeed a quasi-two-dimensional diffusion observed Li$^+$. Therefore, to approximate data, a half-empirical model was used, which was previously presented in paper [21]:

$$R_{1F}^{\mathrm{Li}} = \Delta M \tau \ \ln\left(1 + \frac{1}{(\omega\tau)^2}\right), \tag{1}$$

where τ is determined from the Arrhenius equation:

$$\tau = \tau_0 \exp(E_a/k_B T). \tag{2}$$

The parameters of this model are an amplitude factor ΔM, activation energy for diffusion E_a and a pre-exponential factor from the Arrhenius ratio τ_0. These parameters varied in two frequencies simultaneously to achieve the best approximation of the experimental data. The results of this approximation are shown by solid lines in Figure 5, *a* and 5, *b*. As you can see in Figure 5, *a* and 5, *b* the experimental data is described quite well, which confirms our assumption on the quasi-two-dimensional mechanism of Li$^+$ ion diffusion in $Li_{0.25}TiSe_2$ and $LiTiSe_2$. The corresponding approximation parameters are given in the table.

Summing up the discussion of NMR-measurements in ^{7}Li nucleus in $Li_{0.25}TiSe_2$ and $LiTiSe_2$, we can conclude that diffusion mobility Li$^+$ in both compounds is related to features of the structure of layered dichalcogenides. The available studies of Li$^+$ ion diffusion in Li_xTiSe_2 compounds [18,22,23] predict that this mechanism must be similar to that implemented in the related class of Li_xTiS_2 compounds[24,25]. Based on the fact that Li$^+$ ions in $Li_{0.25}TiSe_2$ and $LiTiSe_2$ occupy only one crystallographically non-equivalent position (1b), where they are octahedrally coordinated with six Se atoms (Figure 1), the most preferable diffusion path Li$^+$ from one octahedral position to the other position may include the intermediate population of the tetrahedral position (2d) [18,22]. Therefore, the elementary act of diffusion process in $Li_{0.25}TiSe_2$ and $LiTiSe_2$, probably, happens according to the $1b \rightarrow 2d \rightarrow 1b$ scheme similar to the case of Li_xTiS_2 [18,25], as shown in Figure 6.

It should be noted that the distance between two adjacent octahedral positions (1b–1b) Li$^+$ in a Van der Waals gap is 3.60 Å, which is quite a long distance for the elementary jump. This fact confirms the assumption on the intermediate population of the tetrahedral position (2d) in process of

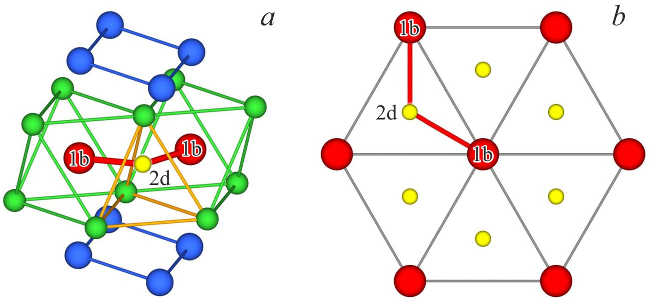

Figure 6. *a*) Schematic image of Li^+ jumps in the crystalline structure of Li_xTiSe_2 from one octahedral position to another one via an intermediate tetrahedral position (red is for Li atoms in the octahedral position, yellow — intermediate tetrahedral 2d position of Li, blue — Ti, green — Se). b) Schematic image of Li^+ jumps via an intermediate tetrahedral position in a lithium sublattice (red is for Li atoms, yellow — intermediate tetrahedral 2d positions Li).

Li^+ diffusion in $Li_{0.25}TiSe_2$ and $LiTiSe_2$. Neglecting any correlations of atomic jumps Li^+, the D diffusion coefficient for the case of quasi-two-dimensional motion may be estimated as follows:

$$D = L^2\tau^{-1}/4, \tag{3}$$

where L — elementary jump length. The value of τ^{-1} jumps of Li^+ ions in both compounds may be obtained at room temperature (297 K) using approximation parameters given in the table, and Arrhenius equation (2); such estimate provides $\tau^{-1}(297\,K) \approx 2.75 \cdot 10^4\,s^{-1}$ for $Li_{0.25}TiSe_2$ and $\tau^{-1}(297\,K) \approx 1.07 \cdot 10^5\,s^{-1}$ for $LiTiSe_2$. If to define length L you use the distance 1b–2d (2.08 Å), we get D (297 K) $\approx 2.98 \cdot 10^{-11}$ cm^2/s for $Li_{0.25}TiSe_2$ and D (297 K) $\approx 1.16 \cdot 10^{-11}$ cm^2/s for $LiTiSe_2$. A small difference in the values of diffusion coefficients may be related to higher activation energy of lithium diffusion in $LiTiSe_2$ (see table). These values may be used to estimate ion conductivity σ from the Nernst–Einstein ratio:

$$\sigma = \frac{nD(Ze)^2}{k_BT}, \tag{4}$$

where n — density of charge carriers per volume unit, and Ze — electric charge of carriers. According to the structural data [13], Li^+ ion density is $n = 3.44 \cdot 10^{21}\,cm^{-3}$ in $Li_{0.25}TiSe_2$ and $n = 1.376 \cdot 10^{22}\,cm^{-3}$ in $LiTiSe_2$. Using the above values, we get the following estimates: σ (297 K)= $6.39 \cdot 10^{-7}$ S/cm for $Li_{0.25}TiSe_2$ and σ (297 K) = $9.96 \cdot 10^{-7}$ S/cm for $LiTiSe_2$. The difference of values may be related to the lower concentration of Li^+ ions in $Li_{0.25}TiSe_2$ structure [13]. The values obtained in this paper may be compared to the results of NMR studies of $Li_{0.7}TiSe_2$ [18]. In the mentioned paper the lithium diffusion activation energy was ~ 370 meV, which is substantially lower than the values we obtained [18]. Such difference in the energy of activation between the related compounds may be due to the fact that concentration of intercalated lithium $Li_{0.7}$ is the most energetically beneficial for ion diffusion. To add, you may compare the D diffusion coefficient values we estimated to the data for the related $LiTiS_2$ compound. The Li^+ diffusion coefficient in a $LiTiS_2$ single crystal was determined by potentiostatic method and made D ($LiTiS_2$) ~ $1.0 \cdot 10^{-8}$ cm^2/s at room temperature [5]. This value is by three orders of magnitude higher than those we determined for $Li_{0.25}TiSe_2$ and $LiTiSe_2$. It follows that lithium diffusion in Li_xTiSe_2 compounds happens much slower than in Li_xTiS_2 compounds [18,26], which seems to be related to a higher activation barrier for lithium diffusion [18].

For activation energy of E_a silver diffusion in Ag_xTiS_2 in paper [27] they proposed a formula that may be used to describe the diffusion in all intercalate compounds, where the intercalant occupies the octahedral position in the Van der Waals gap:

$$E_a = \Delta H_0 - \frac{J}{\alpha + x} \tag{5}$$

Here ΔH_0 — difference of intercalant ion bond enthalpy in octahedral (main) and tetrahedral (excited) chalcogen-coordinated positions; the second member of the right part describes elastic interaction in the form proposed in [28]. According to this representation, the interlayer chemical bond is simulated by a spring with the force of k and length of c_0, which vary in process of intercalation to values K and c_L, respectively. Then the resulting energy per ion will be:

$$\frac{E}{N} = J\frac{x}{\alpha + x}. \quad \text{where} \quad J = \frac{K}{2}(c_L - c_0)^2, \quad \alpha = \frac{K}{k}, \tag{6}$$

x — dimensionless concentration. Since all values in equation (6) are positive, the elastic distortions introduced by an intercalated ion, reduce the activation energy determined by equation (5). Therefore, the decrease of elastic distortions must result in increase of diffusion activation energy. As shown in [29], increase of interlayer distance with the constant ionic radius decreases elastic distortions. Therefore, the increase of the c_0 lattice parameter in $TiSe_2$ compared to this parameter in TiS_2 must lead to the growth of lithium diffusion activation energy in $TiSe_2$. Using the difference of lithium diffusion activation energies in TiS_2 and $TiSe_2$, you can estimate contributions of ΔH_0 and elasticity to the total value E_a. The stiffness of the interlayer bond may be estimated using the value of compressibility in the normal direction to the basal plane. For TiS_2 the compressibility is $\eta_c = 1.46 \cdot 10^{-11}\,Pa^{-1}$ [30], and for $TiSe_2$ $\eta_c = 1.53 \cdot 10^{-11}\,Pa^{-1}$ [31]. As you can see, the stiffness is nearly the same, the difference is not more than 5%. The value J for TiS_2 was estimated as ~ 0.1 eV [28], whereas for $TiSe_2$ it is estimated as $J = 0.435$ eV [27]. Therefore, if the activation energy varied only because of elastic contribution, the difference in E_a values for TiS_2 and $TiSe_2$ would be at least 0.3 eV. In fact, E_a for TiS_2 is estimated from 0.4 eV [32] to 0.45 eV [33], and the difference $E_a(TiSe_2) - E_a(TiS_2)$ is 0.06–0.1 eV. This means that the main change of activation energy is caused by the difference ΔH_0, reflecting the difference in the value of the covalent contribution to the enthalpy of ion bond to the host lattice in the octahedrally and tetrahedrally chalcogen-coordinated positions. You can see that this difference is much less in case of $TiSe_2$ and may be estimated as $0.6-0.66$ eV [27] vs. 0.88 eV in TiS_2. It is evident that this is due to the higher polarizability of selenium compared to sulfur providing for more effective interaction of mobile lithium with chalcogen sublattice in case of $TiSe_2$.

4. Conclusion

Analysis of temperature and frequency dependences of ^{7}Li spin-lattice relaxation rates in lithium-intercalated titanium diselenides $Li_{0.25}TiSe_2$ and $LiTiSe_2$ found diffusion motion of Li^+ ions in these compounds. In the temperature range above 370 K the main contribution to the spin-lattice relaxation rates is made by translational diffusion Li^+. The experimental data on relaxation in both compounds demonstrates the behavior specific for the process of low-dimensional (quasi-two-dimensional) diffusion. This may be related to the structural features of Li_xTiSe_2 lithium diselenides, which consist of Se–Ti–Se layers with Li^+ ions intercalated into Van der Waals cavities between the layers. The maximum rate of ^{7}Li spin-lattice relaxation is observed at frequency of 14.8 MHz at 463 K for $Li_{0.25}TiSe_2$ and 475 K for $LiTiSe_2$. The experimental data for both compounds are satisfactorily described within a half-empirical model for quasi-two-dimensional translational diffusion with activation energy of 501 meV for $Li_{0.25}TiSe_2$ and 509 meV for $LiTiSe_2$. Our estimates of lithium diffusion coefficients at room temperature demonstrated values $D = 2.98 \cdot 10^{-11}\,\mathrm{cm^2/s}$ for $Li_{0.25}TiSe_2$ and $D = 1.16 \cdot 10^{-11}\,\mathrm{cm^2/s}$ for $LiTiSe_2$, which is substantially lower than was obtained for a related compound $LiTiS_2$ [26].

Funding

The study was conducted under the state assignment of the Ministry of Education and Science of Russia for the Institute of Metal Physics, Ural Branch of the Russian Academy of Sciences (Reg. No. NIOKTR 122021000036-3) and the Institute of Solid State Chemistry, Ural Branch of the Russian Academy of Sciences (Reg. No. NIOKTR 124020600047-4).

Conflict of interest

The authors declare that they have no conflict of interest.

References

[1] A.S. Shkvarin, A.I. Merentsov, M.S. Postnikov, E.G. Shkvarina, A.S. Volegov, S.V. Pryanichnikov, P.A. Zayats, A.M. Lebedev, R.G. Chumakov, A.N. Titov. Inorg. Chem. **63**, *2*, 934 (2024).
[2] E.A. Suslov, O.V. Bushkova, E.A. Sherstobitova, O.G. Reznitskikh, A.N. Titov. Ionics **22**, *4*, 503 (2016).
[3] A. Chaturvedi, P. Hu, C. Kloc, Y.-S. Lee, V. Aravindan, S. Madhavi. J. Mater. Chem. A **5**, *37*, 19819 (2017).
[4] A.Yu. Kuznetsova, E.A. Suslov, A.N. Titov. J. Chem. Phys. **160**, *21*, 211103 (2024).
[5] M.S. Whittingham. Prog. Solid State Chem. **12**, *1*, 41 (1978).
[6] M.S. Whittingham. Chem. Rev. **104**, *10*, 4271 (2004).
[7] A.D. Yoffe. Solid State Ionics **9–10**, *1*, 59 (1983).
[8] C. Julien, A. Mauger, A. Vijh, K. Zaghib. Lithium Batteries. Science and Technology. Springer, Berlin (2016). 619 p.
[9] P. Li, X. Zheng, H. Yu, G. Zhao, J. Shu, X. Xu, W. Sun, S.X. Dou. Energy Storage Mater. **16**, 512 (2019).
[10] C. Zhao, D. Wang, R. Lian, D. Kan, Y. Dou, C. Wang, G. Chen, Y. Wei. Applied Surface Science **540**, *1*, 148314 (2021).
[11] C.V. Chandran, P. Heitjans, in: Annual Reports on NMR Spectroscopy / ed. G.A. Webb. Academic Press **89**, 1 (2016).
[12] A.V. Skripov, A.V. Soloninin, O.A. Babanova, R.V. Skoryunov. Molecules **25**, *12*, 2940 (2020).
[13] E.A. Suslov. dis. kand. khim. nauk: 02.00.04. Ekaterinburg (2017). (in Russian).
[14] A. Abragam. The Principles of Nuclear Magnetism. Oxford university press, Oxford (1961). 553 c.
[15] V. Epp, Ö. Gün, H.-J. Deiseroth, M. Wilkening. Phys. Chem. Chem. Phys. **15**, *19*, 7123 (2013).
[16] A.V. Skripov, A.V. Soloninin, M.B. Ley, T.R. Jensen, Y. Filinchuk. J. Phys. Chem. C **117**, *29*, 14965 (2013).
[17] A. Kuhn, P. Sreeraj, R. Pöttgen, H.-D. Wiemhoöfer, M. Wilkening, P. Heitjans. J. Am. Chem. Soc. **133**, *29*, 11018 (2011).
[18] W. Bensch, T. Bredow, H. Ebert, P. Heitjans, S. Indris, S. Mankovsky, M. Wilkening. Prog. in Solid State Chem. **37**, *2*, 206 (2009).
[19] R.G. Barnes, in: Hydrogen in Metals III / ed. H. Wipf. Springer, Berlin (1997). P. 93.
[20] A.V. Soloninin, A.L. Buzlukov, A.V. Skripov, M. Latroche, V. Paul-Boncour. J. of Solid State Chem. **182**, *3*, 586 (2009).
[21] P.M. Richards, in: Physics of Superionic Conductors / ed. M.B. Salamon. Springer, Berlin (1979). P. 141.
[22] C. Ramírez, R. Adelung, R. Kunz, L. Kipp, W. Schattke. Phys. Rev. B **71**, *3*, 035426 (2005).
[23] C. Ramírez, W. Schattke. Surf. Science **482**, 424 (2001).
[24] A. Van der Ven, J.C. Thomas, Q. Xu, B. Swoboda, D. Morgan. Phys. Rev. B **78**, *10*, 104306 (2008).
[25] M. Wilkening, P. Heitjans. Phys. Rev. B **77**, *2*, 024311 (2008).
[26] W. Küchler, P. Heitjans, A. Payer, R. Schöllhorn. Solid State Ionics **70**, 434 (1994).
[27] A.N. Titov. FTT **51**, *4*, 675 (2009). (in Russian).
[28] J.R. Dahn, D.C. Dahn, R.R. Haering. Solid State Commun. **42**, *3*, 179 (1982).
[29] T. Hibma, in: Intercalation Chemistry / ed. M.S. Wittingham, A.J. Jacobsen. Academic Press, London (1982). P. 285–313.
[30] D.R. Allan, A.A. Kelsey, S.L. Clark, R.J. Angel, G.J. Ackland. Phys. Rev. B **57**, 5106 (1998).
[31] A.N. Titov, A.V. Dolgoshein, I.K. Bdikin, S.G. Titova. FTT **42**, *9*, 1567 (2000). (in Russian).
[32] B. Ruprecht, J. Heine, M. Wilkening, S. Indris, J. Wontcheu, W. Bensch, T. Bredow, P. Heitjans. Diffusion Fundamentals **12**, 106 (2010).
[33] R.L. Kleinberg, B.G. Silbernagel. Solid State Communications **36**, 345 (1980).

Translated by M.Verenikina